

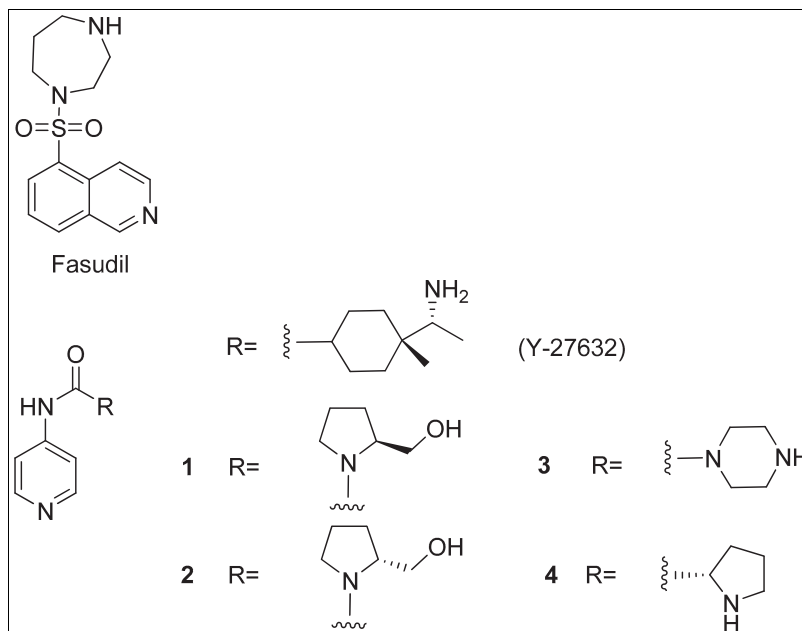
Xinran Wang,^a Ligong Chen,^a Hang Li,^b Changhai Sun,^c Haofei Qi,^a and Donghua Wang^{b*}^aSchool of Chemical Engineering and Technology, Tianjin University, Tianjin 300072, People's Republic of China^bSchool of Pharmaceutical Science and Technology, Tianjin University, Tianjin 300072, People's Republic of China^cTianjin Chase Sun Pharmaceutical Co., Ltd, Tianjin 301700, People's Republic of China

*E-mail: lgchen@tju.edu.cn

Received December 6, 2013

DOI 10.1002/jhet.2238

Published online 00 Month 2014 in Wiley Online Library (wileyonlinelibrary.com).



A series of pyridine Rho kinase inhibitors were designed and synthesized utilizing the ligand-binding pocket model with Y-26732 as the lead compound. These compounds were evaluated on cell lines for their biological activities.

J. Heterocyclic Chem., **00**, 00 (2014).

INTRODUCTION

Rho kinases, namely Rho associated coil kinases, are serine/threonine kinases and are identified as Rho binding protein from bovine brain [1]. They play an important role in a variety of cellular functions such as tumor invasion, cell adhesion, smooth muscle contraction, and formation of focal adhesion fibers [2]. However, the kinases require strict inactivation to prevent spurious cellular signaling; overactivity can lead to cancer or other diseases [3]. So Rho kinases are now regarded as attractive, well-drugable targets [4,5], and they provide new ways of developing therapeutic strategies for the treatment of a number of diseases such as hypertension [6], inflammation [7], cancer [8], and injury caused by ischemia–reperfusion [9], and others [10,11]. Furthermore, some reports have demonstrated that Rho kinase is involved in neurite outgrowth and synaptic plasticity [12,13]. In the injured central nervous system, Rho kinase activation enhances neurite retraction [14], whereas Rho kinase inhibition enhances

axonal regeneration [15]. So, in our work, we focus on screening out Rho kinase inhibitors with significant inhibition activity and neuroprotection.

Rho kinase inhibitors fall into pyridine, isoquinoline, 1*H*-indazole, and phthalimide categories [16]. As the representative of isoquinoline, the first Rho kinase inhibitor is Fasudil (Fig. 1), which was approved in 1995 for the treatment of cerebral vasospasm, a painful and potentially deadly result of subarachnoid hemorrhage [17]. Recently, Y-26732 (Fig. 1), a pyridine derivative, was reported to induce coronary vasodilator actions [18]. Because of its effects *in vivo*, Y-26732 seems important for future clinical applications, so we devoted on synthesizing the Y-26732 analogues to screen out desired Rho kinase inhibitors. The ligand-binding pocket model of the Rho kinase helps us to comprehensively understand and to predict the structure–activity relationship (SAR) of the inhibitors [19]. This model is useful for developing new Rho kinase inhibitors with higher potency and selectivity. The ligand-binding pocket could be divided into three regions, regions A, F,

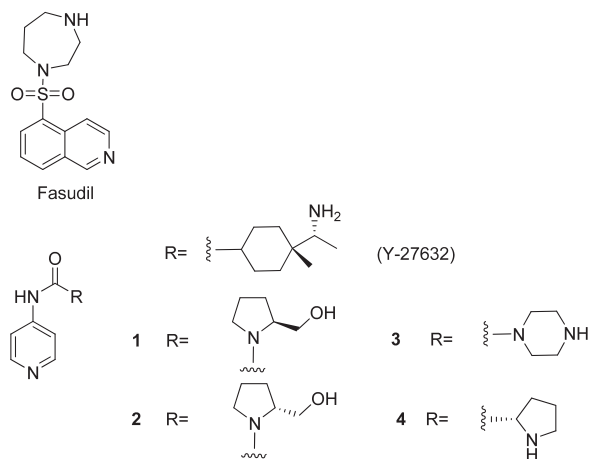


Figure 1. The structures of Fasudil, Y-27632, and target compounds.

and D [19]. Most researchers paid attention to region A [20], whereas region D was overlooked.

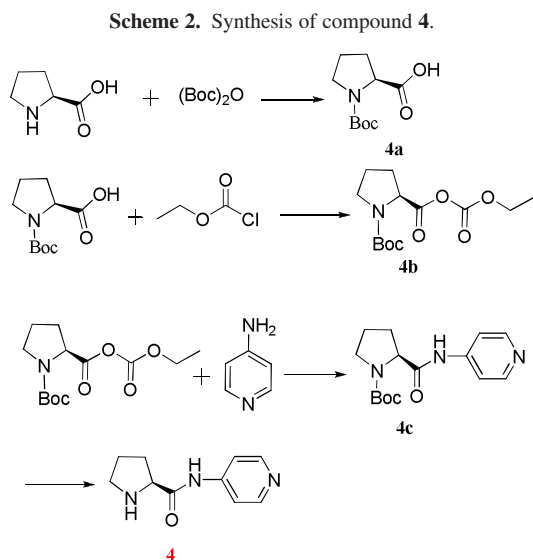
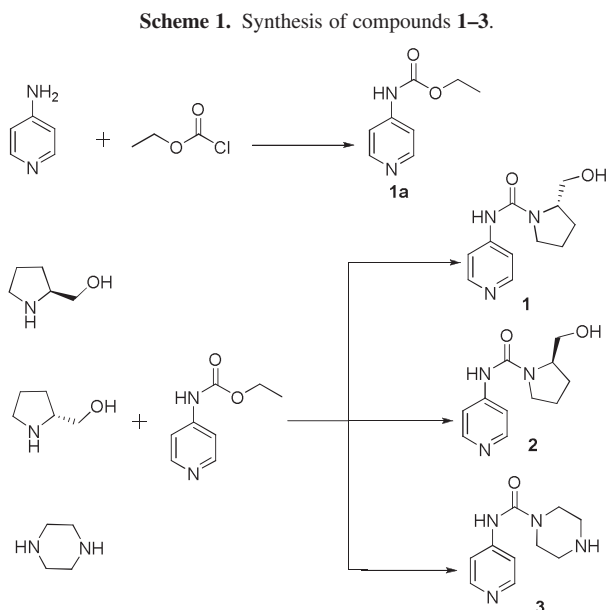
The SAR study demonstrated that modification on the part of Rho inhibitor related with region D could effectively improve the pharmaceutical activity. Therefore, in this article, we summarized our work on a new series of Y-27632 analogues. Compounds **1–4** were designed and synthesized utilizing the ligand-binding pocket model, and their biological activities were evaluated, including Rho kinase inhibitory activities, cell regeneration and synapse formation, cell viability, and cytotoxicity by MTT assay and lactate dehydrogenase (LDH) assay.

CHEMISTRY

In 2004, Takami *et al.* successfully synthesized pyridine Rho kinase inhibitors from isocyanate and 4-aminopyridine. In this article, we tried to synthesize ethyl pyridin-4-ylcarbamate (**1a**) from 4-aminopyridine and ethyl chloroformate via nucleophilic substitution in 87.3% yield [21]. Treatment of Compound **1a** with corresponding amines in the presence of *N*-methylpyrrolidine yielded compounds **1**, **2**, and **3** in 40.7%, 40.6%, and 51.1% yield, respectively (Scheme 1) [22]. Compound **4** was synthesized through the steps shown in Scheme 2 [23].

RESULTS AND DISCUSSION

Considering the chiral structure of Y-27632 that might play an important role for the improvement of biological activity, we introduced L-prolinol and D-prolinol groups to Y-27632, which led to compounds **1** and **2**. Structurally, observing homopiperazine unit in Fasudil, piperazine and pyrrolidine groups were introduced to Y-27632 to yield compounds **3** and **4**. Aimed on exploring the SAR, compounds **1–4** and Fasudil were evaluated for their Rho kinase inhibitory activity, cell regeneration and synapse



formation, and the ability of cell viability and cytotoxicity as shown in the following figures.

Rho kinase inhibitory activity. BV2 cells were treated with Fasudil and compounds **1–4**, respectively, and the Rho kinase inhibitory activity was determined after 24 h by lipopolysaccharide (10 $\mu\text{g}/\text{mL}$). All the results were shown in Figure 2; compounds **3** and **4** display better activity than Fasudil. The inhibiting activity of compounds **1** and **2** are different possibly because of the chirality of binding sites; compound **1** is better than **2** possibly because majority of proteins in the body is in L-configuration. The possibility that contributed to the above phenomenon lies in that if the amino or hydroxyl

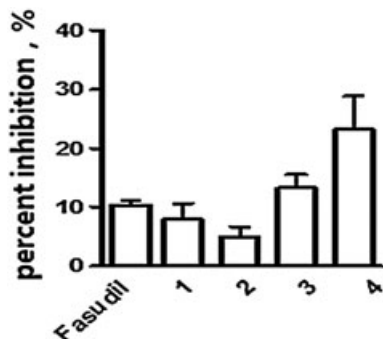


Figure 2. Determination of the activity of the Rho kinase inhibitors.

group is a binding site, compounds **3** and **4** are less steric hindrance to facilitate a combination with Rho kinase and the nucleophilic ability of amino group is higher than the hydroxyl group.

The neuroprotection of Rho kinase inhibitor. Determination of the ability of synapse formation. Generally speaking, synapse formation is beneficial to cell regeneration. Here, we took the test on primary neurons; that is to say, we

tested the recovery of nerve cells. These cells were processed by phosphate-buffered saline (PBS), Fasudil, and compounds **1–4** for 24 h. As seen in Figure 3, the synapse formation was more effectively enhanced by compounds **1–4** than Fasudil.

On the basis of the above experiment, we carried out the experiments with BV2 cells under the same conditions (Fig. 4). In contrast to PBS, the synapse is the most evident that was treated with compound **2**, Fasudil can lead the cells to death on the contrary, and the rest of the compounds have no obvious effects on synapse formation.

We further carried out the quantitative determination of the average length of synapses (BV2 cells) in the presence of Fasudil and compounds **1–4** (Fig. 5). The cells treated with compound **4** formed the obvious synapse, Fasudil comes after, but the shape of cells treated by Fasudil seems poor.

Determination of cell viability. Cell viability was assessed by measuring the cellular metabolism of MTT. In order to test whether these compounds were effective to promote cell viability, first, MTT on primary neurons was used to examine the cell viability in the presence of

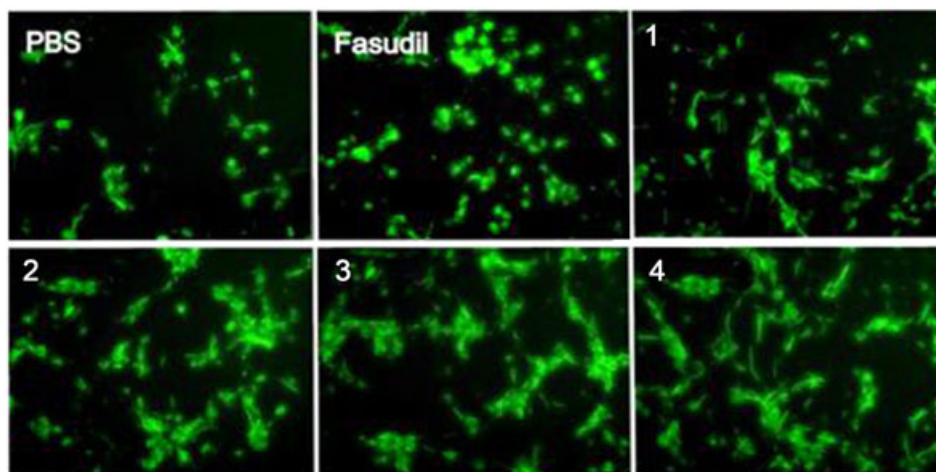


Figure 3. Determination of cell regeneration and synapse formation (primary neurons) in the presence of Fasudil and compounds **1–4**. [Color figure can be viewed in the online issue, which is available at www.interscience.wiley.com.]

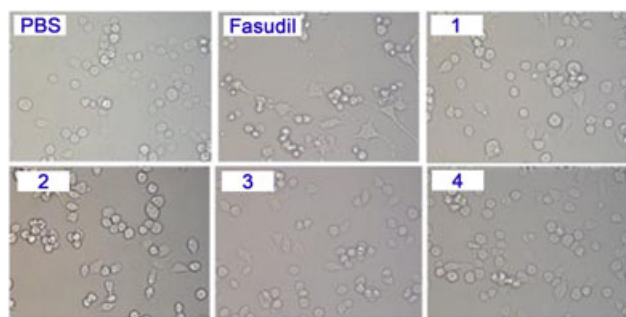


Figure 4. Determination of cell regeneration and synapse formation (BV2 cells) in the presence of Fasudil and compounds **1–4**. [Color figure can be viewed in the online issue, which is available at www.interscience.wiley.com.]

these compounds. Cell viability was expressed as the neuroprotection of these compounds. As shown in Figure 6, we examined the influence of these compounds with 1, 5, 15, and 50 $\mu\text{g/mL}$ on the cell viability. Comparing with PBS, cell viability in the presence of all the new compounds appears to be slightly increased. Among them, the influence of compound **3** is most obvious. The obtained results indicated that Fasudil in high concentration (50 $\mu\text{g/mL}$) could obviously inhibit the cell viability. By contrast, cell viability treated by compound **3** do not change in low concentration, whereas at medium and high concentration, cell viability is obviously enhanced.

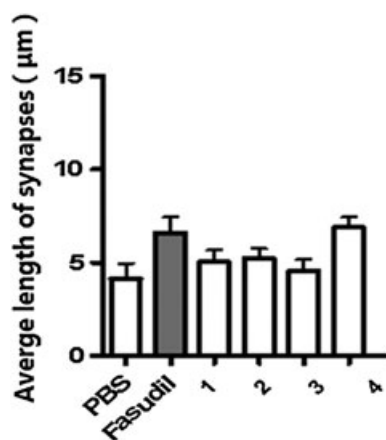


Figure 5. Determination of the length of synapse in the presence of Fasudil and compounds 1–4.

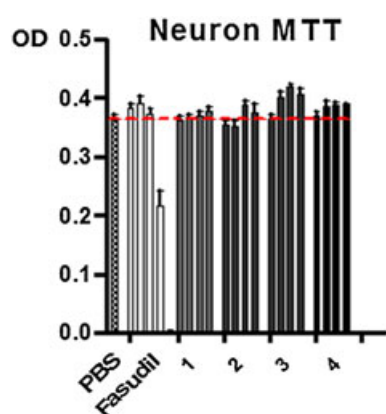


Figure 6. Determination of cell viability (primary neurons) in the presence of Fasudil and compounds 1–4. [Color figure can be viewed in the online issue, which is available at www.interscience.wiley.com.]

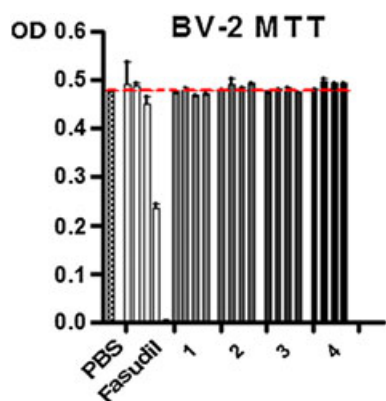


Figure 7. Determination of cell viability (BV2 cells) in the presence of Fasudil and compounds 1–4. [Color figure can be viewed in the online issue, which is available at www.interscience.wiley.com.]

As seen in Figure 7, BV2 cells were examined in the presence of these compounds by MTT assay. These cell lines were treated with increasing concentrations (1, 5, 15, and

50 µg/mL) of each compound. With PBS as baseline, Fasudil have slight inhibitory activity. All new compounds show a slight increase or no influence. Fasudil could obviously inhibit the viability at increased concentration (50 µg/mL), whereas the other compounds show no influence.

Determination of cytotoxicity. The cytotoxicity of these compounds to primary neurons was determined by LDH assay; the results are summarized in Figure 8. The primary neurons were treated with all compounds in 24 h. The concentrations are 1, 5, 15, and 50 µg/mL. In comparison to PBS, compound 4 exhibited the lowest cell toxicity. Compound 3 took seconds. As seen in Figure 8, cytotoxicity was obviously increased in cell cultures containing Fasudil at high concentration; however, the cytotoxicity of compounds 3 and 4 decreases with the increase of concentration. They could possibly protect the primary neurons to some degree.

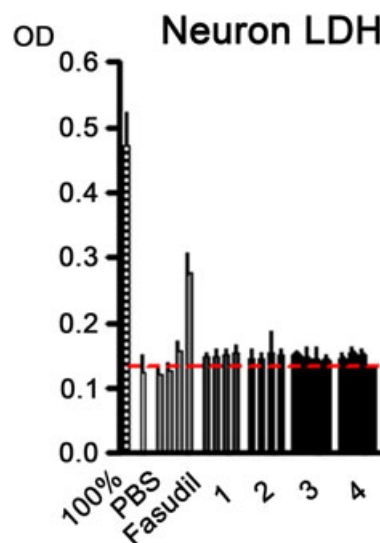


Figure 8. Determination of cytotoxicity (primary neurons) in the presence of Fasudil and compounds 1–4. [Color figure can be viewed in the online issue, which is available at www.interscience.wiley.com.]

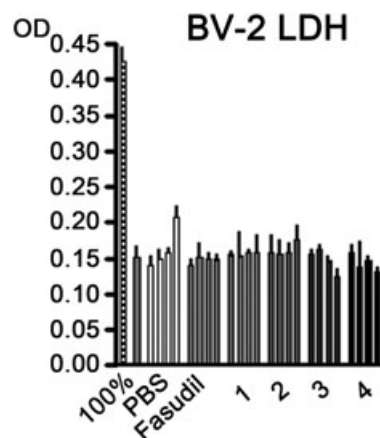


Figure 9. Determination of cytotoxicity (BV2 cells) in the presence of Fasudil and compounds 1–4.

As seen in Figure 9, BV2 cells were chosen for further testing, and the cytotoxicity of these compounds (1, 5, 15, and 50 $\mu\text{g/mL}$) was tested. Compound **4** has the lowest cytotoxicity, and Fasudil has the highest. The rest of the compounds show no obvious toxicity. Compounds **3** and **4** in high concentration (50 $\mu\text{g/mL}$) could reduce the cytotoxicity.

The results of the above study provide evidence of the neuroprotective effects of these Rho kinase inhibitors. Compounds **3** and **4** modulate the neurite growth and protect neurons from cytotoxicity-induced cell death.

CONCLUSION

In summary, we successfully synthesized four pyridine derivatives. Their biological activities were evaluated, including Rho kinase inhibitory activity, cell regeneration and synapse formation, cell viability, and cytotoxicity by the MTT and LDH methods. Compound **4** exhibited higher inhibitory activities of Rho kinase than Fasudil and modulated neurite growth and protect neurons from cytotoxicity-induced cell death, and compound **3** was less effective than compound **4**. Observing the structures of compounds **1**, **2**, **3**, and **4**, if the amino group is a binding site, compounds **3** and **4** is less stereo-hindrance to facilitate a combination with the Rho kinase and the nucleophilic ability of amino group is higher than the hydroxyl group. Thus, it is inferred that electron effects or steric effects may be the crucial factors to affect the results. The activity of compounds **1** and **2** are different possibly because of the chirality of binding sites, and compound **1** is better than **2** possibly because majority of the proteins in the body is in L-configuration. Further studies are necessary to clarify the inference. Compound **4** will be under further study as a drug candidate.

EXPERIMENTAL

All reagents were used as purchased from commercial suppliers without further purification unless otherwise noted. Solvents were dried and purified according to standard procedures before use. The course of reactions was monitored by TLC (silica gel GF254s). Flash chromatography was performed using 200–300-mesh silica gel. ^1H and ^{13}C NMR spectra were recorded on an INOVA 400/600-Hz spectrometer with TMS as an internal standard. HR-MS was recorded on MicrOTOF-Q II (Bucker Daltonics Inc., Billerica, MA).

(S)-2-(Hydroxymethyl)-N-(pyridin-4-yl)pyrrolidine-1-carboxamide (1). To a solution of 4-aminopyridine (3.76 g, 39.95 mmol) in CH_2Cl_2 (50 mL) at 0°C was added triethylamine (4.85 g, 47.94 mmol) and ethyl chloroformate (4.34 g, 39.95 mmol). The resulting mixture was allowed to warm to room temperature overnight and then was concentrated. The solid products were slurried with water. The reaction mixture was adjusted to $\text{pH}=5-6$ by 5% hydrochloric acid. Then, the aqueous phase was extracted by ethyl acetate (50 mL \times 3). The ethyl acetate phases were combined, dried over MgSO_4 , and concentrated to afford 5.80 g white solid (**1a**), 87.3% yield. ^1H

NMR (CDCl_3 , 600 MHz) δ : 10.02 (s, 1H), 8.56 (d, $J=6.2$ Hz, 2H), 7.63 (d, $J=6.2$ Hz, 2H), 4.33 (q, $J=7.1$ Hz, 2H), 1.38 (t, $J=7.1$ Hz, 3H). ^{13}C NMR (CDCl_3 , 150 MHz) δ : 154.3, 150.2, 147.3, 113.3, 61.8, 14.8.

Compound (**1a**) was added into a solution of L-prolinol in 1,4-dioxane with *N*-methylpyrrolidine as catalyst. The mixture was reflux for 24 h, and then the residue was concentrated. The residue was purified by silica gel column (ethyl acetate/methanol = 5/1, v/v) to afford (**1**) 2.23 g, 40.7% yield. Mp: 154.5–155.1 $^\circ\text{C}$. ^1H NMR (CDCl_3 , 600 MHz) δ : 8.16 (d, $J=6.0$ Hz, 2H), 7.28 (d, $J=6.0$ Hz, 2H), 3.97 (s, 1H), 3.58–3.69 (m, $J=121.5$ Hz, 5H), 1.77–2.02 (m, 4H), 1.57 (s, 1H). ^{13}C NMR (CDCl_3 , 150 MHz) δ : 155.77, 149.20, 147.99, 113.07, 66.77, 60.11, 47.16, 29.18, 23.55. HR-MS (ESI), calcd $\text{C}_{11}\text{H}_{15}\text{N}_3\text{O}_2$: $[\text{M}+\text{H}]^+$ m/z : 221.1243; found: 221.1246.

Compounds 2 and 3 were synthesized by the same method. (R)-2-(Hydroxymethyl)-N-(pyridin-4-yl)pyrrolidine-1-carboxamide (2). 40.6% yield, mp: 154.1–155.7 $^\circ\text{C}$. ^1H NMR (CDCl_3 , 600 MHz) δ : 8.13 (d, $J=6.1$ Hz, 2H), 7.26 (d, $J=6.1$ Hz, 2H), 3.94 (m, 1H), 3.71–3.47 (m, 4H), 3.28 (s, 1H), 1.95–1.74 (m, 4H), 1.54 (s, 1H). ^{13}C NMR (CDCl_3 , 150 MHz) δ : 155.71, 149.03, 148.15, 113.07, 66.73, 60.11, 47.14, 29.19, 23.52. HR-MS (ESI), calcd $\text{C}_{11}\text{H}_{15}\text{N}_3\text{O}_2$: $[\text{M}+\text{H}]^+$ m/z : 221.1243; found: 221.1246.

N-(Pyridin-4-yl)piperazine-1-carboxamide (3). 51.1% yield, mp: 196.3–197.1 $^\circ\text{C}$. ^1H NMR (CD_3OD , 600 MHz) δ : 8.24 (d, $J=6.0$ Hz, 2H), 7.48 (d, $J=6.0$ Hz, 2H), 3.51 (s, 4H), 2.83 (s, 4H). ^{13}C NMR (CD_3OD , 150 MHz) δ : 156.47, 150.28, 149.94, 114.96, 46.31, 45.85. HR-MS (ESI), calcd $\text{C}_{10}\text{H}_{15}\text{ClN}_4\text{O}$: $[\text{M}+\text{H}]^+$ m/z : 207.1246; found: 207.1252.

(R)-N-(Pyridin-4-yl)pyrrolidine-2-carboxamide (4). The solution of di-*tert*-butyl dicarbonate (9.09 g, 41.69 mmol) in THF (30 mL) was added to a mixture of L-proline (4.00 g, 34.74 mmol) and sodium hydroxide solution (2 mol/L, 30 mL) at 0°C . The mixture was stirred at room temperature for 12 h and then concentrated. The rest of the reaction mixture was adjusted to $\text{pH}=2-3$ by 5% hydrochloric acid solution. Then, the aqueous phase was extracted by ethyl acetate (50 mL \times 3). The ethyl acetate phases were combined, dried over MgSO_4 , and concentrated to give Boc-L-proline 7.10 g, 95.0% yield.

The solution of Boc-L-proline (7.10 g, 33.00 mmol) and triethylamine (3.34 g, 33.00 mmol) in dry THF (100 mL) was cooled to 0°C . Under stirring, ethyl chloroformate (3.58 g, 33.00 mmol) was introduced into the solution in 15 min. After the mixture had been stirred for a further 30 min at 0°C , 4-aminopyridine (3.10 g, 33.00 mmol) was added slowly over 15 min. This reaction mixture was stirred for 1 h at 0°C , 16 h at room temperature, and heated at reflux for 3 h. The mixture was subsequently diluted with ethyl acetate and triethylamine and then filtrated. The resulting residue was dissolved in ethyl acetate, washed with saturated aqueous ammonium chloride, dried over MgSO_4 , filtered, and concentrated to give the compound 8.17 g yellow liquid (**4c**), 72.9% yield. Trifluoroacetic acid (10 mL) was added dropwise to the compound (**4c**) in dichloromethane (20 mL) at 0°C . The mixture was stirred at room temperature for 12 h, then adjusting to $\text{pH}=12-13$ by 2 mol/L sodium hydroxide solution. Then, the aqueous phase was extracted by dichloromethane (50 mL \times 3). The dichloromethane phases were combined, dried over MgSO_4 , and concentrated to give 5.14 g yellow solid (**4**), 95.7% yield. mp: 209.1–209.5 $^\circ\text{C}$. ^1H NMR (CD_3OD , 600 MHz) δ : 8.39 (d, $J=6.6$ Hz, 2H), 7.68 (d, $J=6.6$ Hz,

2H), 3.91 (m, 1H), 3.06–3.01 (m, 2H), 2.23 (m, 1H), 1.90 (m, 1H), 1.78 (m, 2H). ^{13}C NMR (CD_3OD , 150 MHz) δ : 175.96, 150.97, 147.55, 115.18, 62.38, 48.12, 32.06, 27.10. HR-MS (ESI), calcd $\text{C}_{10}\text{H}_{13}\text{N}_3\text{O}$: $[\text{M} + \text{H}]^+$ m/z : 192.1137; found: 192.1144.

BIOLOGICAL METHODS

Materials. Animals: Female C57BL/6 mice, 8–10 weeks old, were purchased from Vital River Laboratory Animal Technology Co. Ltd (Beijing, China) and housed in the animal care facilities of Shanghai Second Medical University under pathogen-free conditions according to the Institutional Animal Care and Use Committee guidelines.

Primary culture of neurons: On 16–18 days of their pregnancy, mice were sacrificed, and their brains were removed under aseptic conditions. Suspensions of mononuclear cells from brains were prepared by grinding the organ through a 40- μm nylon mesh in medium. Then, the suspension was centrifuged and resuspended in 2% B27 Neurobasal-A supplemented with 10% fetal bovine serum. Cells were then seeded at $1 \times 10^6/\text{mL}$ in PLL-treated flask and incubated at 37°C with 5% CO_2 . After 7 days, the neurons were detected with MAP-2 monoclonal antibodies and used for the experiments mentioned previously.

Culture of BV2 cells: rat BV2 cell lines were bought from American Type Culture Collection, subcultured by Baoguo Xiao' laboratory. BV2 cells initially were adjusted to $1 \times 10^5/\text{mL}$ into DMEM plate (10 cm^2) with 10% fetal bovine serum and subcultured at 37°C with 5% CO_2 .

Rho kinase inhibition assay. This experiment was carried out with BV2 cells. The Rho kinases were activated by lipopolysaccharide, and then Fasudil and compounds 1–4 were added to the activated Rho kinase. The Rho kinase activities of the above samples were determined by EAE model.

The Enzyme Linked Immunosorbent Assay Kit (ELISAK), CycLex Co. Ltd, #CY-1160, was purchased from Japan.

Cell regeneration and synapse formation assay. After 7–8 days of cultivation, original generation neurons were washed with 0.1 mol/L PBS three times, and then the cells were incubated with MAP-2 monoclonal antibodies at 4°C overnight. The next day it was washed with 0.1 mol/L PBS again, added secondary antibodies labeled by fluorescent at 37°C, washed again with 0.1 mol/L PBS after 2 h, sealed piece by 50% glycerol, and observed under fluorescence microscope. Then, we used Image-Pro Plus to measure and calculate the average length of synaptic cells. The average length of synapses of BV2 cells could be observed directly.

MTT assay. MTT assay is used to detect cell survival and growth methods. The basic principles are as follows: the mitochondria dehydrogenase in the living cells can restore yellow brominated [3-(4,5-dimethylthiazol-2-yl)-2,5-diphenylterazolium bromide, MTT] to formazan,

which is violet and aqueous insoluble. The formazan can exit the living cell; however, the dead cells have no such function. So we dissolved the formazan of the cells in dimethyl sulfoxide, and their optical densities were measured with the wavelength at 490 nm by Universal Microplate Spectrophotometer, which could indirectly reflect the number of living cells.

LDH assay. The LDH assay is the determination of concentration of LDH and is based on the measurement of the cytoplasmic enzyme released when the plasma membrane is damaged. Adding the synthesized compounds into the purified LDH antibodies, washing thoroughly, and developing by tetramethylbenzidine (TMB), we found that TMB turned into blue over LDH. They eventually turned into yellow under the acidic conditions. Their optical densities were measured with the wavelength at 490 nm by Universal Microplate Spectrophotometer. The extent of LDH release was expressed as the percentage of the total release, that is, the release of LDH after cell lyses with 1% Triton.

Statistical analysis. All the experiments were repeated three times. Data are presented as mean \pm SD. Data were analyzed using one-way analysis of variance with a post hoc test (multiple comparison test) that can be used to determine the significant differences between groups. Significance was accepted at $P < 0.05$.

Acknowledgment. The authors would like to acknowledge Professor Baoguo Xiao of Fudan University for the biological activity evaluations in this article.

REFERENCES AND NOTES

- [1] Ishizaki, T.; Maekawa, M.; Fujisawa, K.; Okawa, K.; Iwamatsu, A.; Fujita, A.; Watanabe, N.; Saito, Y.; Kakizuka, A.; Morii, N.; Narumiya, S. *EMBO J* 1996, 15, 1885.
- [2] Olson, M. F. *Curr Opin Cell Biol* 2008, 20, 242.
- [3] Breitenlechner, C.; Gafel, M.; Hidaka, H.; Kinzel, V.; Huber, R.; Engh, R. A.; Bossemeyer, D. *Structure* 2003, 11, 1595.
- [4] Schmitz, A. A. P.; Govek, E. E.; Bottner, B.; Aelst, L. V. *Exp Cell Res* 2000, 261, 1.
- [5] Chen, Y. T.; Vojtkovsky, T.; Fang, X. G.; Pocas, J. R.; Grant, W.; Handy, A. M. W.; Schroter, T.; LoGrasso, P.; Bannister, T. D.; Feng, Y. B. *Med Chem Commun* 2011, 2, 73.
- [6] Force, T.; Kuida, K.; Namchuk, M.; Parang, K.; Kyriakis, J. M. *Circulation* 2004, 109, 1196.
- [7] LoGrasso Philip, V.; Feng, Y. *Curr Top Med Chem* 2009, 9, 704.
- [8] Wong, C. C. L.; Wong, C. M.; Tung, E. K. K.; Man, K.; Ng, I. O. L. *Hepatology* 2009, 49, 1583.
- [9] Dong, M.; Yan, B. P.; Yu, C. M. *Cardiovasc Hematol Agents Med Chem* 2009, 7, 322.
- [10] Nishimura, Y.; Itoh, K.; Yoshioka, K.; Tokuda, K.; Himeno, M. *Pathol Oncol Res* 2003, 9, 83.
- [11] Kamai, T.; Tsujii, T.; Arai, K.; Takagi, K.; Asami, H.; Ito, Y.; Oshima, H.; *Clin Cancer Res* 2003, 9, 2632.
- [12] Mueller, B. K.; Mack, H.; Teusch, N. *Nat Rev Drug Discov* 2005, 4, 387.
- [13] Da Silva, J. S.; Dotti, C. G. *Nat Rev Neurosci* 2002, 3, 694.

- [14] Govek, E. E.; Newey, S. E.; Aelst, L. V. *Genes Dev* 2005, 19, 1.
- [15] Fournier, A. E.; Takizawa, B. T.; Strittmatter, S. M. *J Neurosci*, 2003, 23, 1416.
- [16] Kamai, T.; Yamanishi, T.; Shirataki, H.; Takagi, K.; Asami, H.; Ito, Y.; Yoshida, K. I. *Clin Cancer Res*, 2004, 10, 4799.
- [17] Ono-Saito, N.; Niki, I.; Hidaka, H. *Pharmacol Ther* 1999, 82, 123.
- [18] Renteria, L. S.; Austin, M.; Lazaro, M.; Andrews, M. A.; Lustina, J.; Raj, J. U.; Ibe, B. O. *Cell Prolif* 2013, 46, 563.
- [19] Iwakubo, A. T. M.; Okada, Y.; Kawata, T.; Odai, H.; Takahashi, N.; Shindo, K.; Kimura, K.; Tagami, Y.; Miyake, M.; Fukushima, K.; Inagaki, M.; Amano, M.; Kaibuchi, K.; Iijima, H. *Bioorg Med Chem* 2004, 12, 2115.
- [20] Shen, M. Y.; Yu, H. D.; Li, Y. Y.; Li, P. X.; Pan, P. C.; Zhou, S. Y.; Zhang, L. L.; Li, S.; Lee, S. M. Y.; Hou, T. J. *J Mol BioSyst* 2013, 9, 1511.
- [21] Borgens, R. B.; Shi, R.; Byrn, S. R.; Smith, D. T. *World Pat.*, 2004052291, 2004. *Chem Abstr* 2004, 141, 47362.
- [22] Gallou, I.; Eriksson, M.; Zeng, X. Z. H.; Senanayake, C.; Farina, V. *J Org Chem* 2005, 70, 6960.
- [23] Kinsella, M.; Duggan, P. G.; Lennon, C. M. *Tetrahedron: Asymmetry* 2011, 22, 1423